Fracture Testing of a Self-Healing Polymer Composite*

E.N. Brown,[1] N.R. Sottos[1] and S.R. White[2]
[1]Department of Theoretical and Applied Mechanics
[2]Department of Aeronautical and Astronautical Engineering
University of Illinois Urbana-Champaign
Urbana, IL 61801

Abstract

Inspired by biological systems in which damage triggers an autonomic healing response, we have developed a polymer composite material that can heal itself when cracked. This paper summarizes the self-healing concept for polymeric composite materials and investigates fracture mechanics issues consequential to the development and optimization of this new class of materials. The self-healing material under investigation is an epoxy matrix composite, which incorporates a microencapsulated healing agent that is released upon crack intrusion. Polymerization of the healing agent is triggered by contact with an embedded catalyst. The effects of size and concentration of catalyst and microcapsules on fracture toughness and healing efficiency are investigated. In all cases the addition of microcapsules significantly toughens the neat epoxy. Once healed, the self-healing polymer recovers as much as 90% of its virgin fracture toughness.

* Submitted for publication in *Experimental Mechanics: An International Journal* (2001)

Introduction

Fracture of the skeletal structure in biological systems provides an excellent model for developing a synthetic healing process for structural materials. For a bone to heal, nutrients and undifferentiated stem cells must be delivered to the fracture site and sufficient healing time must elapse.[1] The healing process consists of multiple stages of deposition and assembly of material,[2] as illustrated in Fig. 1. The network of blood vessels in the bone is ruptured by the fracture event, initiating autonomic healing by delivering the components needed to regenerate the bone.

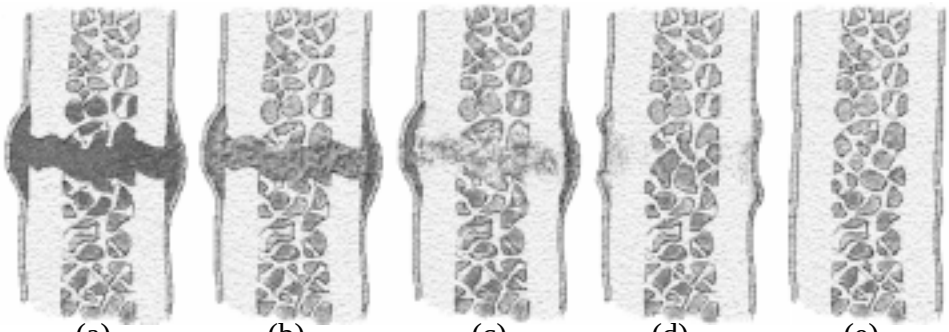

Fig. 1–Healing stages of bone; (a) internal bleeding, forming a fibrin clot, (b) development of unorganized fiber mesh, (c) calcification of the fibrocartilage, (d) calcification converted into fibrous bone, (e) transformation into lamellar bone

In recent research, White *et al.*[3] have developed a self-healing polymer that mimics many of the features of a biological system. The self-healing system, shown schematically in Fig. 2, involves a three-stage healing process, accomplished by incorporating a microencapsulated healing agent and a catalytic chemical trigger in an epoxy matrix. Conclusive demonstration of self-healing was obtained with a healing agent based on the **r**ing-**o**pening **m**etathesis **p**olymerization (ROMP) reaction. Dicyclopentadiene (DCPD), a highly stable monomer with excellent shelf life, was encapsulated in microcapsules with a thin shell made of urea formaldehyde. A small volume fraction of microcapsules was dispersed in a common epoxy resin along with the Grubbs ROMP catalyst, a living catalyst that remains active after triggering the polymerization. The embedded microcapsules were shown to rupture in the presence of a crack and to release the DCPD monomer into the crack plane. Contact with the embedded Grubbs catalyst initiated polymerization of the DCPD and rebonded the crack plane. Crack healing efficiency was assessed by adopting a measurement of the ability to recover fracture,[4]

$$\eta = \frac{K_{\mathrm{I}c_{\mathrm{healed}}}}{K_{\mathrm{I}c_{\mathrm{virgin}}}}, \tag{1}$$

where $K_{\mathrm{I}c_{\mathrm{virgin}}}$ is the fracture toughness of the virgin specimen and $K_{\mathrm{I}c_{\mathrm{healed}}}$ is the fracture toughness of the healed specimen. Fracture test results using the ROMP-based healing

system revealed that on average 60% of the fracture toughness was recovered in the healed samples.

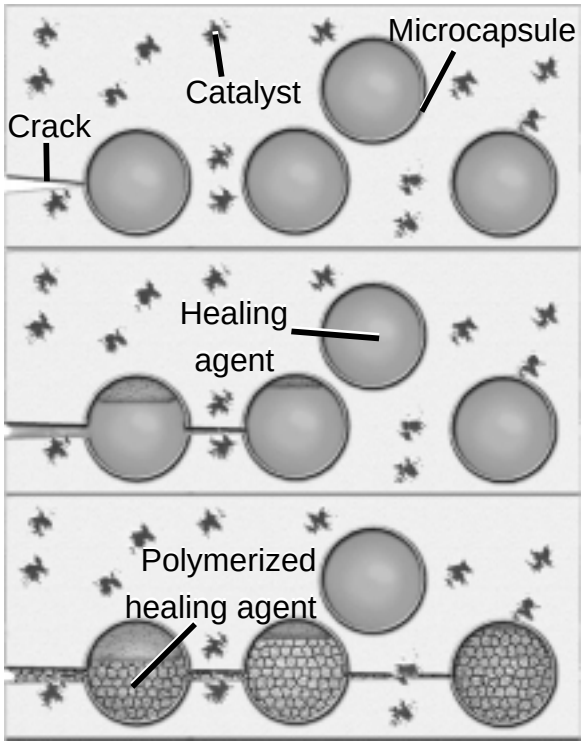

Fig. 2–Self-healing concept for a thermosetting polymer

Crack-healing phenomena have been discussed in the literature for several types of synthetic materials including glass, concrete, asphalt, and a range of polymers.[4-15] While these previous works were successful in repairing or sealing cracks, the healing was not self-initiated and required some form of manual intervention (*e.g.* application of heat, solvents, or healing agents). Others have proposed a tube-delivery concept for self-repair of corrosion damage in concrete and cracks in polymers.[16,17] Albeit conceptually interesting, the introduction of large hollow tubes in a brittle matrix material cause stress concentrations that weaken the material and beneficial healing may be difficult to realize.

In contrast, the microcapsule concept developed by White *et al.*[3] is particularly elegant, practical, and promising for the healing of brittle thermosetting polymers. In this paper, we present a comprehensive experimental investigation of the correlative fracture and healing mechanisms of this self-healing system. Effects of microcapsule concentration, catalyst concentration, and healing time are studied with a view towards improving healing efficiency.

Experimental Procedure

Using the protocol established by White *et al.*[3], we measured healing efficiency by carefully controlled fracture experiments for both the virgin and the healed material. These tests utilize a tapered double-cantilever beam (TDCB) geometry, which ensures

controlled crack growth along the centerline of the brittle specimen. The TDCB fracture geometry, developed by Mostovoy *et al.*,[18] provides a crack-length-independent measure of fracture toughness

$$K_{Ic} = 2P_c\sqrt{\frac{m}{b_n b}}, \tag{2}$$

which requires knowledge of only the critical fracture load P_c and geometric terms. The specimen and crack widths are given by b and b_n, respectively. The geometric term m is defined by the theoretical relation

$$m = \frac{3a^2}{h(a)^3} + \frac{1}{h(a)}, \tag{3}$$

or is determined experimentally by the Irwin–Keys[19] method as

$$m = \frac{Eb}{8}\frac{\mathrm{d}C}{\mathrm{d}a}, \tag{4}$$

where E is the Young's modulus, C is the compliance, and $h(a)$ is the specimen height profile. For the TDCB sample geometry, the healing efficiency, Eq. 1, is rewritten as

$$\eta = \frac{P_{c\,\mathrm{healed}}}{P_{c\,\mathrm{virgin}}}. \tag{5}$$

TDCB Specimen

Valid profiles for a TDCB fracture specimen are determined by finding a height profile that when inserted into Eq. 3 yields a constant value of m over a desired range of crack lengths. Height profiles that provide exact solution are complex curves, but are approximated with linear tapers.[12,18,20,21] In the current work, the TDCB geometry developed and verified by Beres[20] is adopted. Relevant dimensions are shown in Fig. 3.

When the taper angle is small, a crack propagating in a brittle material exhibits a propensity to deflect significantly from the center line. Failure commonly occurs as arm break-off. To ensure that fracture follows the desired path, side grooves were incorporated into the TDCB geometry. Addition of side grooves is valid for the TDCB geometry, as there is no restriction that b and b_n have the same value. Stable crack propagation with maximum crack width b_n was obtained by selecting a groove with 45° internal angle.[22]

A series of 18 fracture toughness tests were performed on pure epoxy (EPON® 828/DETA) TDCB specimens with crack lengths ranging from 20 to 37 mm to determine m from Eq. 4. A plot of compliance *versus* crack length was constructed and a linear fit made, extrapolating a constant value of dC/da. The fracture toughness of the neat epoxy and the geometric constant m were measured to be 0.55 MPa $m^{1/2}$ and 0.6 mm^{-1},

respectively. This experimental value of *m* is in excellent agreement with the value predicted by the finite-element method[20].

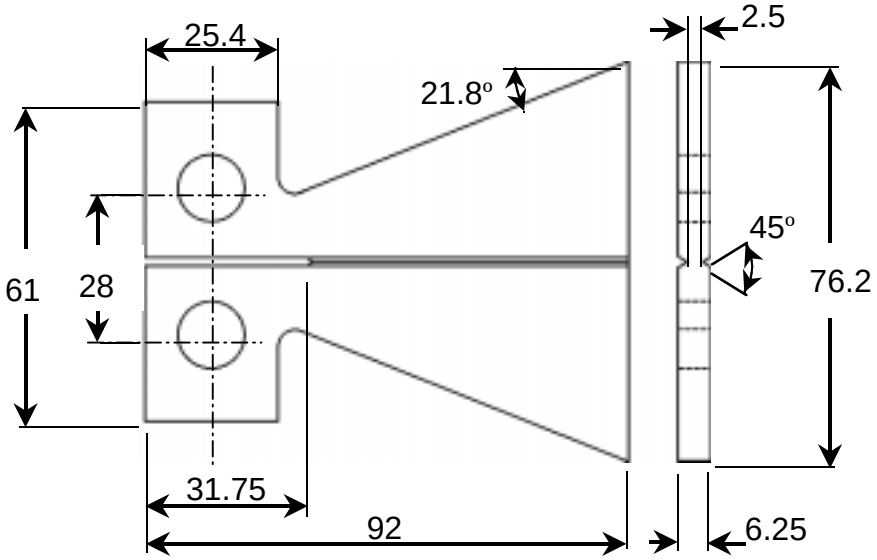

Fig. 3–Tapered double-cantilever beam (TDCB) geometry (dimensions in mm)

Sample Preparation and Test Method

Samples were prepared by mixing EPON® 828 epoxy resin with 12 pph Anacmine® DETA curing agent. The epoxy mixture was degassed, poured into a closed silicone rubber mold, and cured for 24 hours at room temperature, followed by 24 hours at 30°C. After curing, a sharp pre-crack was created by gently tapping a razor blade into the molded starter notch in the samples. To facilitate investigation of the effects of the constituents of the self-healing system, varying weight percent of Grubbs catalyst and/or microcapsules were mixed into the resin prior to pouring.

Three types of experiment are conducted: the self-healing *in situ* tests and two types of control. The first type of control, referred to as reference samples, consists of neat epoxy without embedded catalyst. Reference samples are tested to failure and then manually healed by injection of DCPD monomer that is premixed with catalyst. Reference tests remove the variables associated with DCPD delivery and the embedding of Grubbs catalyst. The second control, referred to as self-activated samples, consists of epoxy with embedded catalyst but no microcapsules. Self-activated samples are tested to failure and then healed by manual injection of DCPD monomer into the crack plane. This intermediate-level control enables investigation of the embedded catalyst, without the variability of DCPD delivery through microencapsulation. The third type of sample is the fully self-contained, or *in situ*, system. *In situ* samples contain both the microencapsulated healing agent and Grubbs catalyst, enabling them to self-heal after fracture. Urea-formaldehyde microcapsules encapsulating DCPD monomer were manufactured. The emulsion microencapsulation method used is outlined in White *et al*.[3] Table 1 summarizes the different sample types.

TABLE 1–SAMPLE TYPES

Sample type	Epoxy (EPON® 828:DETA)	Grubbs catalyst	Microencapsulated healing agent
Reference control	100:12	–	0-25 wt%
Self-activated control	100:12	0-5 wt%	–
In situ self-healing	100:12	2.5 wt%	5-10 wt%

Fracture specimens were tested under displacement control, using pin loading and a 5μm/s displacement rate. Samples were tested to failure, measuring compliance and peak load. For the reference samples, 0.03 ml of premixed DCPD monomer and Grubbs catalyst was injected into the crack plane, prior to crack closing. For the case of self-activated samples, 0.03 ml of DCPD monomer was injected into the crack plane, which is subsequently allowed to close. *In situ* samples were unloaded, allowing the crack faces to come back into contact. After a sufficient time for healing efficiency to reach a steady value, the samples were retested. For the majority of experiments, retesting was performed after 48 hours. Values of fracture toughness and the subsequent healing efficiency were calculated. A representative load–displacement curve is shown in Fig. 4 for the *in situ* healing case. Virgin fracture is brittle in nature, while the healed fracture exhibits prolonged stick-slip.

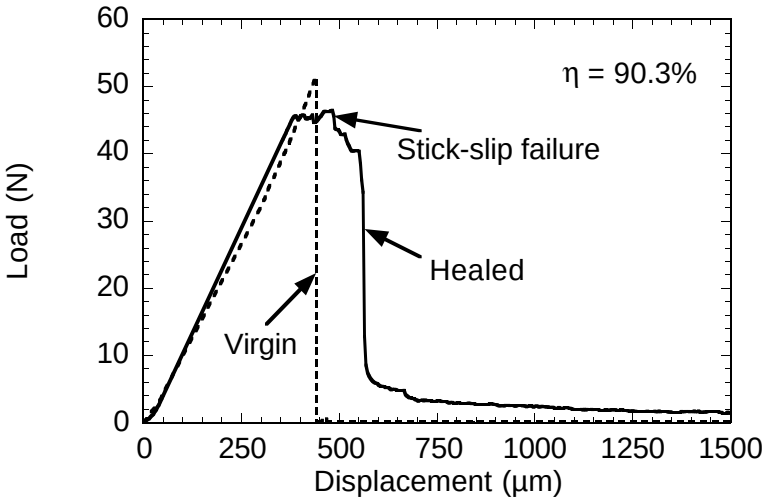

Fig. 4–Representative load–displacement curve for an *in situ* sample with 2.5 wt% Grubbs and 5 wt% capsules

Healing of the Reference System

Potential of the healing system is first investigated via fracture-toughness testing of reference samples. Following a virgin fracture test, approximately 0.03 ml of mixed DCPD monomer and catalyst was injected into the crack plane. An advantage of the Grubbs catalyst/DCPD monomer system is its catalytic reaction. Unlike two-part

polymerization reactions, such as epoxy, which require a precise stoichiomerty ratio, the catalyst drives the reaction even with minimum concentration.

Catalyst Concentration

The effect of the ratio of Grubbs catalyst to DCPD monomer was investigated by measuring the healing efficiency in four sets of samples with catalyst to DCPD ratios of 2, 4.4, 10, and 40 g/l. Each set consisted of 18 samples. As shown in Table 2, the level of healing efficiency increased as the concentration of catalyst was increased, while the gel time decreased exponentially, taking approximately 600 s, 235 s, 90 s and 25 s, respectively.

TABLE 2–DEPENDENCE OF HEALING EFFICIENCY IN REFERENCE SAMPLES ON CATALYST CONCENTRATION

Concentration	Fracture toughness (MPa $m^{1/2}$)		
Grubbs:DCPD (g:l)	Virgin	Healed	Healing efficiency
40:1	0.55 ± 0.05	0.71± 0.08	Full heal
10:1	0.56 ± 0.04	0.61± 0.09	Full heal
4.4:1	0.55 ± 0.05	0.53± 0.10	97 ± 15%
2:1	0.54 ± 0.04	0.45± 0.08	84 ± 8%

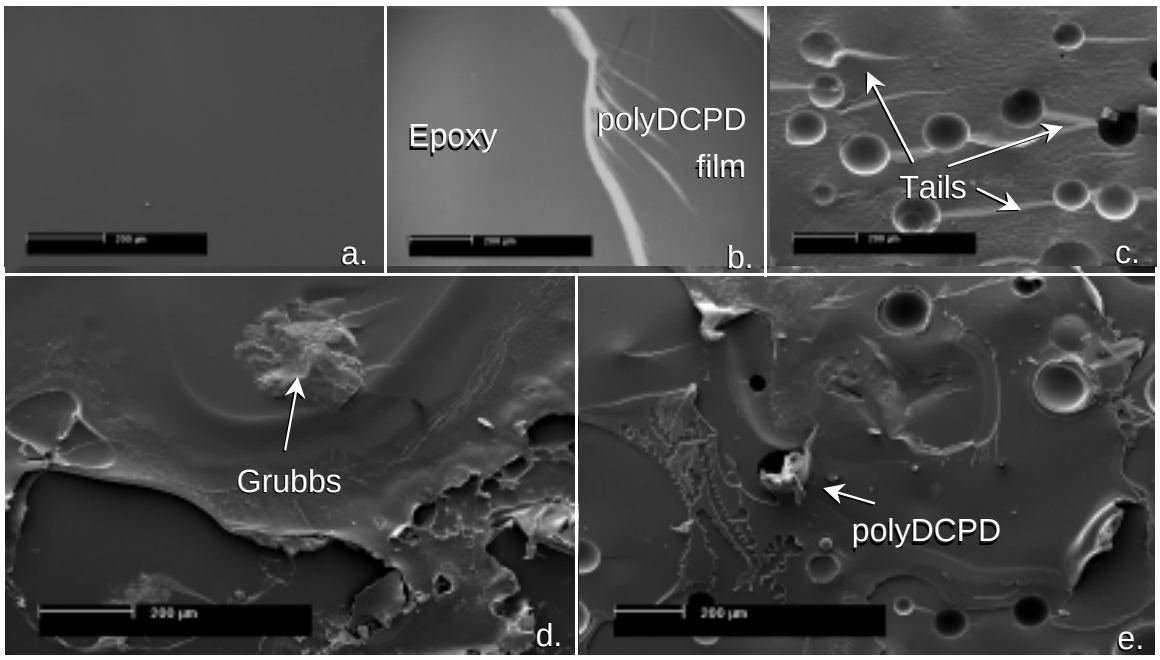

Fig. 5–Crack plane ESEM images: (a) neat epoxy, (b) polyDCPD separation from bulk epoxy, (c) reference sample (10 wt% capsules) showing tails related to the crack pinning toughening mechanism, (d) self-activated (2.5 wt% Grubbs catalyst) and (e) *in situ* samples sample (10 wt% capsules and 2.5 wt% catalyst)

Investigation of the fracture planes highlights two phenomena: fracture in pure epoxy results in locally smooth surfaces down to micron length scales (Fig. 5a), and fracture in the healed material occurs as separation between the bulk epoxy and polyDCPD film (Fig. 5b). It is believed that the increased healing efficiency is due to changes in the chemical kinetics and thermodynamics with increased catalyst concentration. Shorter cure times reduce the time required for healing efficiency to reach a steady value, and serve to prevent diffusion and evaporation of DCPD from the crack plane. The ability of the healed reference sample to obtain full healing (healing efficiency = 100%) indicates excellent adhesion between the polymerized DCPD and the epoxy.

Microcapsule Concentration

Reference samples were also used to study the influence of microcapsule concentration on the fracture of the virgin and healed epoxy. Reference samples containing 0% to 25% by weight of microcapsules (ca. 180 μm diameter) were tested to failure and healed manually. As observed earlier in the literature for the addition of rigid particles,[23,24] the virgin fracture toughness of the material increased significantly with increasing concentration of microcapsules, as shown in Fig. 6. A maximum is achieved at 15 wt% capsule concentration. This toughening is due to a classic crack pinning mechanism. Observation of the fracture surface in Fig. 5c shows clear evidence of the characteristic tails that indicate crack pinning.

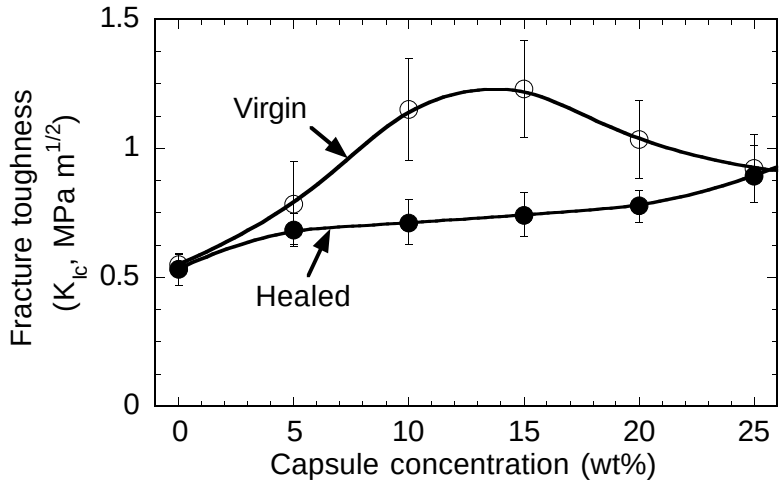

Fig. 6–Virgin and healed fracture toughness dependence on capsule concentration

Healing agent from the microcapsules was allowed to evaporate from the crack plane. The reference samples were then injected with a 4.4 g/l mixture of Grubbs catalyst and DCPD monomer. Healed fracture toughness demonstrated minimal dependence on capsule concentration over a range of 5 to 20% by weight. For capsule concentrations close to the value that yields a maximum for the virgin fracture toughness (~ 15 wt%), a local minimum in healing efficiency occurs due to the minimal gains in healed fracture toughness, illustrated in Fig 7. For capsule concentration of 25 wt% and greater near perfect healing is obtained. However, as the capsule concentration increases the

manufacture of samples becomes more difficult due to increased viscosity of the uncured resin.

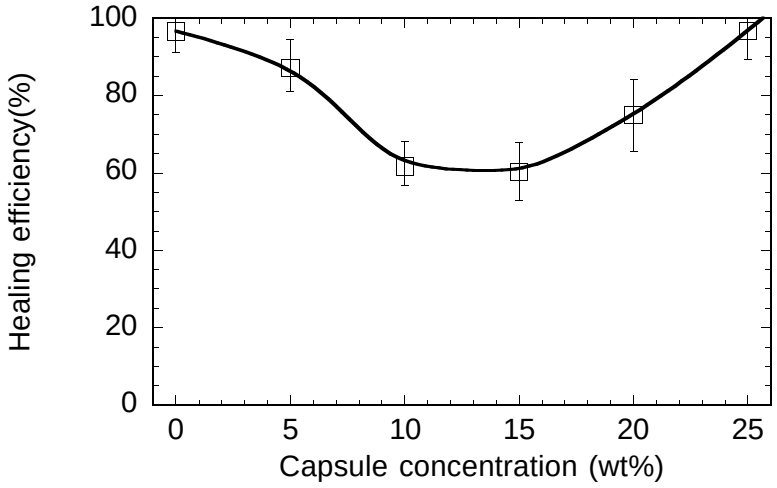

Fig. 7–Healing efficiency dependence on capsule concentration

Healing of the Self-Activated System

The Grubbs catalyst, which is the trigger mechanism for the polymerization of the healing agent, is a fine purple powder with a propensity to form small clumps. From chemical investigation of the interactions between the catalyst and the epoxy system it has been shown that contact of the catalyst during manufacture with the DETA curing agent can degrade the catalyst.[26] The availability of active catalyst is dependent on the order of mixing the catalyst, resin, and curing agent, the catalyst particle size, and the amount of catalyst added. These parameters are investigated with self-activated samples.

Mixing Order

Chemical investigation using proton NMR shows that Grubbs catalyst retains its activity in the presence of the EPON® 828/DETA system during curing. However, contact with only the DETA curing agent causes rapid deactivation of the catalyst. To ascertain the optimal mixing sequence of the three components (EPON® 828/12pph DETA/ 2.5 wt% Grubbs catalyst) to retain the activity of the catalyst and maximize healing efficiency, we manufactured six self-activated samples for each of the three possible sequences. In each case, the first two components were mixed and degassed for 5 minutes. The third component was then integrated and degassed for an additional 5 minutes. Results are summarized in Table 3. Virgin fracture toughness values were statistically unchanged for the three mixing sequences. The healed fracture toughness values and, in turn, the efficiency of healing indicated the importance of mixing order. Mixing the catalyst and DETA curing agent first results in no measurable healing. Failure to recover fracture toughness was interpreted as an indication that the catalyst was extensively deactivated. As shown in Table 3, the other two mixing orders had little effect on the healing efficiency.

TABLE 3–DEPENDENCE OF HEALING EFFICIENCY IN REFERENCE SAMPLES ON MIXING ORDER

Mixing order	Fracture toughness (MPa $m^{1/2}$) Virgin	Healed	Healing efficiency
(EPON® 828 + DETA) + Grubbs	0.73 ± 0.06	0.45 ± 0.8	63 ± 6%
(EPON® 828 + Grubbs) + DETA	0.75 ± 0.05	0.45± 0.09	60 ± 6%
(DETA + Grubbs) + EPON® 828	0.76 ± 0.07	0	0%

Catalyst Particle Size

The size of the Grubbs catalyst particles also influences the behavior of the virgin and healed composite. To determine the size distribution of catalyst that provides the maximum healing efficiency, we ground a sample of catalyst to provide a powder with particle diameters of less than 1mm; the distribution of particle sizes is shown in Fig. 8. Sets of six self-activated samples were manufactured with 2.5 wt% of catalyst with particle sizes of less than 75 μm, 75–180 μm, 180–355 μm, and 355–1000 μm. As illustrated in Fig. 9, both the virgin and healed fracture toughness values increase as the catalyst particle size increases. In the virgin material, the catalyst particles serve as a toughening mechanism through crack pinning,[27] as shown in Fig. 5d. In the healed material, the competing effects of smaller particles provide improved dispersion—and thus availability of catalyst in the crack plane for polymerization of DCPD—and of larger particles providing a reduced surface-area-to-volume ratio for the catalyst. The smaller surface-area-to-volume ratio is believed to reduce the opportunity for DETA curing agent to react with the Grubbs catalyst. Poor healing efficiency was obtained for small particles due to low healed fracture toughness. Large particles do not yield high healed fracture toughness coterminous with their high virgin fracture toughness, also obtaining poor healing efficiency. The highest healing efficiency corresponds to catalyst particle size of 180–355 μm.

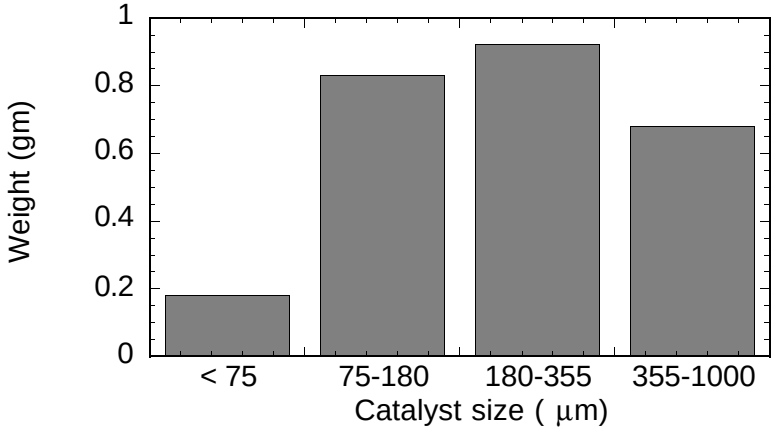

Fig. 8–Particle size distribution of Grubbs catalyst following grinding

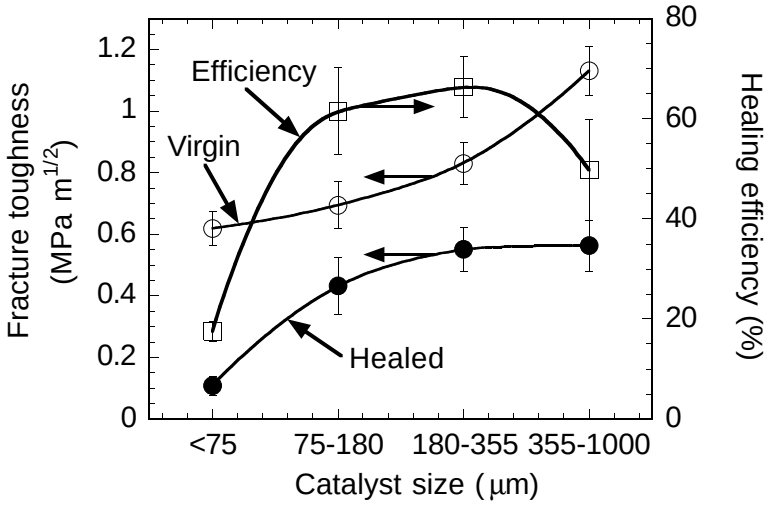

Fig. 9–Dependence of fracture toughness and healing efficiency on catalyst particle size

Catalyst Concentration

To establish the catalyst concentration that provides for high healing efficiency without diminishing virgin fracture toughness, we manufactured six sets of self-activated TDCB samples with Grubbs catalyst concentration from 0 to 4 wt%. Each set consisted of six samples. Virgin and healed fracture toughness values and the corresponding healing efficiencies were measured (Fig. 10). The healed fracture toughness increases with the addition of catalyst. As more catalyst is added, however, the relative gain in healed fracture toughness for each additional increment decreases. For addition of catalyst beyond 3 wt%, the virgin fracture toughness begins to decreases. Although a high healing efficiency results at these high catalyst concentrations, gains are due to diminution of the virgin properties. At high catalyst concentration, scatter in the data is dramatically increased.

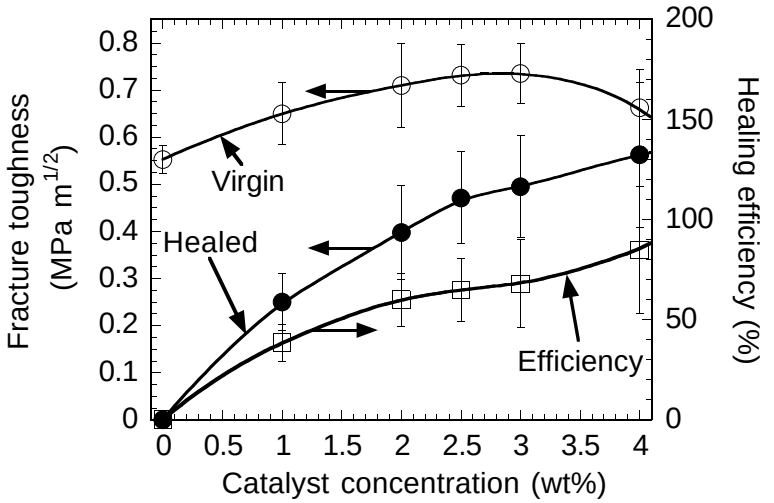

Fig. 10–Healing efficiency as a function of catalyst concentration

Self-Healing of the *In Situ* System

The ultimate goal of this research is the development of a self-healing polymer composite. To achieve this goal, microencapsulated DCPD monomer and Grubbs catalyst were incorporated into an *in situ* sample. The effect of microcapsule size on healing efficiency and the evolution of healed fracture toughness over time were investigated using *in situ* samples with 2.5 wt% Grubbs catalyst and 10 wt% of DCPD monomer encapsulated microcapsules. The findings of these studies and the results presented above were used to optimize the healing system through choice of catalyst and microcapsule concentration.

Microcapsule Size

Three sets of samples were manufactured with 180 ± 40 μm, 250 ± 80 μm and 460 ± 80 μm diameter capsules. When fracture occurred, DCPD monomer was observed to fill the crack plane of the TDCB specimen. Variation in the healed fracture toughness was small, with a trend for increased toughness with decreased capsule diameter, as shown in Fig. 11. Divergence of healing efficiency was governed by the virgin fracture toughness, which increased significantly with decreased capsule diameter. The self-healed specimens with 460 μm diameter capsules exhibited the greatest healing efficiency, recovering 63% of virgin load on average. Investigation of the crack planes revealed that all the microcapsules fractured, releasing the encapsulated healing agent. In Fig. 5e, all the capsules on the fracture plane are fractured with no mounds or protruding shell material representative of debonding.

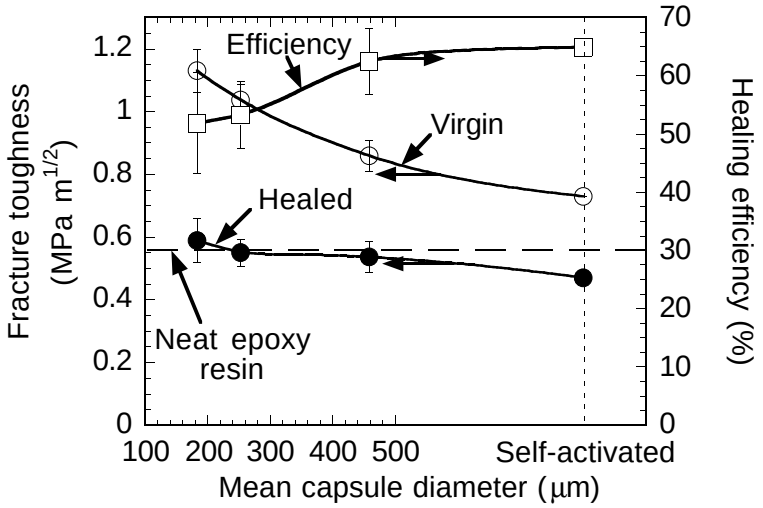

Fig. 11–Influence of microcapsule size on fracture toughness and healing efficiency

Development of Healing Efficiency

The healing efficiencies presented thus far have been measured after waiting 48 hr from the virgin test. This time was chosen to ensure sufficient time for healing. Previous

research on healing of thermoplastics[4,10,11] showed that healing efficiency is strongly tied to time. A series of 28 *in situ* samples was manufactured with 10 wt% of 180 μm diameter capsules and 2.5 wt% of catalyst. The virgin fracture tests were performed in rapid succession with the exact time of the fracture event noted for each specimen. Healed fracture tests were performed at time intervals ranging from 10 min to 72 hr. The resulting healing efficiencies are plotted *versus* time in Fig. 12. A significant healing efficiency developed within 25 minutes, which closely corresponds to the gelation time of the polyDCPD. Steady-state values were reached within 10 hr.

Microcapsule Concentration

In earlier work on this self-healing system,[3,28] it was perceived that the ability to deliver sufficient healing agent could be a limiting factor to healing efficiency. Microcapsule concentration was chosen to be 10 wt% to maximize DCPD delivery, while retaining near-maximum virgin fracture toughness. For the range of microcapsule sizes investigated in Fig. 11, reducing the available healing agent by a factor of seven does not significantly reduce healed fracture toughness, while excess DCPD was observed for all capsule sizes. The data in Fig. 6 for reference samples indicates that a reduction in concentration from 10 to 5 wt% has minimal impact on the observed healed fracture toughness. By reducing the capsule concentration, the virgin fracture toughness can be optimized to yield near perfect healing. A set of six *in situ* samples was manufactured with 5 wt% of 180 μm diameter capsules and 2.5 wt% of catalyst. An average healing efficiency of 85 ± 5% was measured. The relative healing efficiencies of neat epoxy and the *in situ* system with 10 wt% and 5 wt% microcapsules are shown in Fig. 13, illustrating the successful development of an optimized self-healing system.

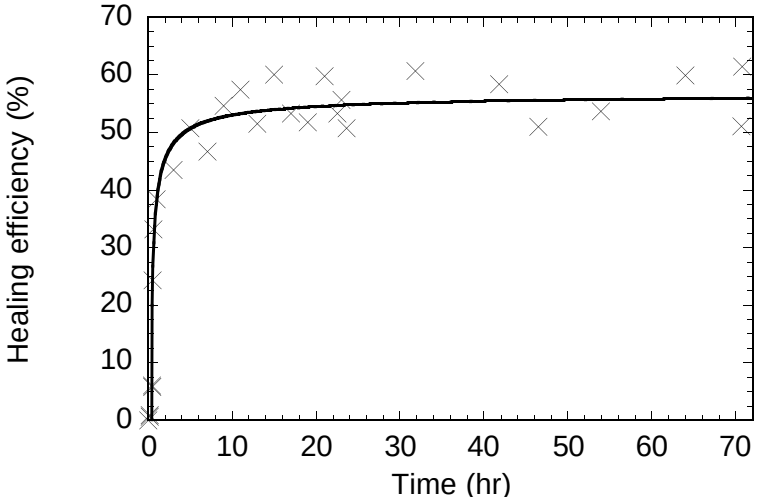

Fig. 12–Development of healing efficiency

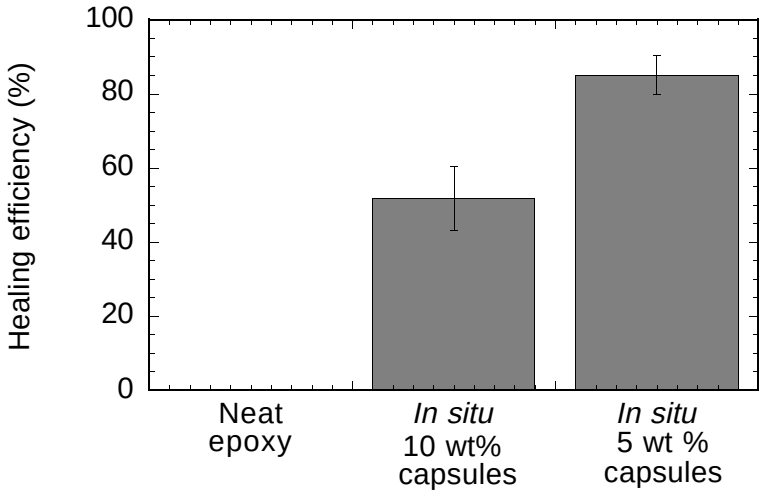

Fig. 13–Comparison of *in situ* healing efficiency for different capsule concentrations (2.5 wt% catalyst)

Conclusions

Use of a tapered double-cantilever beam fracture geometry provided an accurate method to measure the fracture behavior and healing efficiency of self-healing polymer composites and to compare with appropriate controls. Virgin fracture properties of the polymer composite are improved due to crack pinning by microcapsules and catalyst particles. The size and concentration of catalyst were shown to have a significant impact on the virgin properties of the composite and the ability to catalyze the healing agent. The highest healing efficiency was obtained with 180–355 μm catalyst particles. Catalyst concentrations greater than 2.5 wt% provided diminishing gains in healed fracture toughness. Significant loss of virgin fracture toughness was observed for catalyst concentration above 3%. The catalyst was found to remain active following the curing process, given that it was not first mixed with the DETA curing agent. Addition of microcapsules, up to 15 wt%, served to increase the virgin toughness. Capsule size had a direct influence on the volume of DCPD monomer released into the crack plane, but over the range of capsule sizes investigated, healing efficiency was not restricted by lack of healing agent. Maximum healing efficiency was obtained within 10 hours of the fracture event. By optimizing the concentrations of catalyst and microcapsules, we increased the healing efficiency of the system to over 90%.

Acknowledgments

The authors gratefully acknowledge the support of the University of Illinois Critical Research Initiative Program, AFOSR Aerospace and Materials Science Directorate Mechanics and Materials Program, and Motorola Labs, Motorola Advanced Technology Center, Schaumburg Ill. Special thanks are extended to Dr. A. Skipor of Motorola Labs for his continuing support and suggestions. The authors would also like to thank Prof. J.S. Moore and Prof. P.H. Geubelle and graduate students M.R. Kessler and S.R. Sriram for technical support and helpful discussions. Undergraduate B. Lung was extremely

helpful in the preparation of TDCB samples. Electron microscopy was performed in the Imaging Technology Group, Beckman Institute, of the University of Illinois at Urbana-Champaign, with the assistance of S. Robinson.

References

1. Caplan, A.I., "*Bone Development, Cell and Molecular Biology of Vertebrate Hard Tissues", Ciba Foundation Symposium* 136, John Wiley & Sons, 3-16 (1988).

2. Albert, S.F., "*Electrical Stimulation of Bone Repair*," *Clinical Podiatric Medical Surgery*, **8** (4), 923-935 (1981).

3. White, S.R., Sottos, N.R., Geubelle, P.H., Moore, J.S., Kessler, M.R., Sriram, S.R., Brown, E.N., and Viswanathan, S., "*Autonomic healing of polymer composites*," *Nature*, **409**, 794-797 (2001).

4. Wool, R. P., and O'Conner, K. M., "*A Theory of Crack Healing in Polymers*," *Journal of Applied Phys*ics, **52**, 5953-5963 (1982).

5. Sukhotskaya, S.S. Mazhorava, and V.P., Terekhin, Yu N., "*Effect of Autogenous Healing of Concrete Subjected to Periodic Freeze Thaw*," *Hydrotechnical Construction*, **17** (6), 295-296 (1983).

6. Clear, C.A., "*The Effect of Autogenous Healing upon Leakage of Water through Cracks in Concrete*," *Cement and Concrete Association*, Wexham Spring, May (1985).

7.Edvardsen, C., "*Water Permeability and Autogenous Healing of Cracks in Concrete*," *ACI Materials Journal*, **96** (4), 448-454 (1999).

8. Kim, Y.R. and Little, D., "*Evaluation of Self-Healing in Asphalt Concrete by Means of the Theory of Nonlinear Elasticity*," *Transp. Res Rec*., no. 1228, 198-210 (1989).

9. Stavrinidis, B. and Holloway, D.G., "*Crack Healing in Glass*," *Journal of the American Ceramic Society*, **53**, 486-489 (1970).

10. Jud, K. and Kausch, H.H., "*Load transfer through chain molecules after interpentration at interfaces*," *Polymer Bulletin*, **1**, 697-707 (1979).

11. Kausch, H.H. and Jud, K., "*Molecular Aspects of Crack Formation and Healing in Glassy Polymers*," *Rubber Processing and Applications*, **2**, 265-268 (1982).

12. Jung, D., "*Performance and Properties of Embedded Microspheres for Self-Repairing Applications*," MS Thesis, University of Illinois at Urbana-Champaign, (1997).

13. Hegeman, A., "*Self-repairing polymers, repair mechanisms and micromechanical modeling*," MS Thesis, University of Illinois at Urbana-Champaign, (1997).

14. D.Jung, A. Hegeman, N.R. Sottos, P.H. Geubelle, and S.R. White, "Self-healing composites using embedded microspheres," *The American Society for Mechanical Engineers (ASME)*, **MD-80**, 265-275 (1997).

15. Zako, M. and Takano, N., "Intelligent material Systems Using Epoxy Particles to Repair Microcracks and Delamination Damage in GFRP," Journal of Intelligent Material Systems and Structures, **10**, 836-841 (1999).

16. Dry, C., "*Procedures developed for self-repair of polymeric matrix composite materials*," *Composite Structures*, **35**, 263-269 (1996).

17. Motuku, M., Vaidya, U.K., and Janowski, G.M., "*Parametric studies on self-repairing approaches for resin infusion composites subjected to low velocity impact*," *Smart Materials and Structures*, **8**, 623-638 (1999)

18. Mostovoy, S., Crosley P.B., and Ripling, E.J., "*Use of Crack-Line Loaded Specimens for measuring Plain-Strain Fracture Toughness*," *Journal of Materials*, **2** (3), 661-681 (1967).

19. Irwin, G.R. and Kies, J.A., "*Critical Energy Rate Analysis of Fracture Strength*," American Welding Society Journal, **33,** 193-s-198-s (1954).

20. Beres, W., Ashok, K.K., and Thambraj, R., "*A Tapered Double-Cantilever-Beam Specimen Designed for Constant-K Testing at Elevated Temperatures*," *Journal of Testing and Evaluation*, **25**, 536-542 (1997).

21. Meiller, M., Rocje, A.A., and Sautereau, H., "*Tapered Double-Cantilever-Beam Test Used as a Practical Adhesion Test for Metal/Adhesive/Metal Systems*," *Journal of Adhesion ScienceI, **13**, 773-788 (1999).*

22. Marcus, H.L. and Sih, G.C., "*A Crackline-Loaded Edge-Crack Stress Corrosion Specimen*," *Engineering Fracture Mechanics*, **3**, 453-461 (1971).

23. Evans, A.G., "*The Strength of Brittle Materials Containing Second Phase Dispersions*," *The Philosophical Magazine*, **26** (6), 1327-1344 (1972).

24. Broutman, L.J. and Sahu, S., "*The Effect of Interfacial Bonding on the Toughness of Glass Filled Polymers*," *Materials Science Engineering*, **8**, pp. 98-107 (1971).

25. Sancaktar, E. and Gomatam, R., 2001, "*A Study on the Effects of Surface Roughness on the Strength of Single Lap Joints*," *Journal of Adhesion Science and Technology*, **15** (1), 97-117 (2001).

26. Sriram, S., Personal Communication, Department of Chemistry, University of Illinois at Urbana-Champaign (1999).

27. Lange, F.F., "*The Interaction of a Crack Front with a Second-phase Dispersion*," *The Philosophical Magazine*, **22** (179), 983-992 (1970).

28. Brown, E.N. and Sottos, N.R., "*Performance of Embedded Microspheres for Self-Healing Polymer Composites*,"*Society of Experimental Mechanics* IX International Congress on Experimental Mechanics, 563-566 (2000).

List of Recent TAM Reports

No.	*Authors*	*Title*	*Date*
901	Fried, E., and A. Q. Shen	Supplemental relations at a phase interface across which the velocity and temperature jump—*Continuum Mechanics and Thermodynamics* **11**, 277–296 (1999)	Mar. 1999
902	Paris, A. J., and G. A. Costello	Cord composite cylindrical shells: Multiple layers of cords at various angles to the shell axis	Apr. 1999
903	Ferney, B. D., M. R. DeVary, K. J. Hsia, and A. Needleman	Oscillatory crack growth in glass—*Scripta Materialia* **41**, 275–281 (1999)	Apr. 1999
904	Fried, E., and S. Sellers	Microforces and the theory of solute transport—*Zeitschrift für angewandte Mathematik und Physik* **51**, 732–751 (2000)	Apr. 1999
905	Balachandar, S., J. D. Buckmaster, and M. Short	The generation of axial vorticity in solid-propellant rocket-motor flows—*Journal of Fluid Mechanics* (submitted)	May 1999
906	Aref, H., and D. L. Vainchtein	The equation of state of a foam—*Physics of Fluids* **12**, 23–28 (2000)	May 1999
907	Subramanian, S. J., and P. Sofronis	Modeling of the interaction between densification mechanisms in powder compaction—*International Journal of Solids and Structures*, in press (2000)	May 1999
908	Aref, H., and M. A. Stremler	Four-vortex motion with zero total circulation and impulse—*Physics of Fluids* **11,** 3704-3715	May 1999
909	Adrian, R. J., K. T. Christensen, and Z.-C. Liu	On the analysis and interpretation of turbulent velocity fields—*Experiments in Fluids* **29**, 275–290 (2000)	May 1999
910	Fried, E., and S. Sellers	Theory for atomic diffusion on fixed and deformable crystal lattices—*Journal of Elasticity* **59**, 67–81 (2000)	June 1999
911	Sofronis, P., and N. Aravas	Hydrogen induced shear localization of the plastic flow in metals and alloys—*European Journal of Mechanics/A Solids* (submitted)	June 1999
912	Anderson, D. R., D. E. Carlson, and E. Fried	A continuum-mechanical theory for nematic elastomers—*Journal of Elasticity* **56**, 33–58 (1999)	June 1999
913	Riahi, D. N.	High Rayleigh number convection in a rotating melt during alloy solidification—*Recent Developments in Crystal Growth Research* **2**, 211–222 (2000)	July 1999
914	Riahi, D. N.	Buoyancy driven flow in a rotating low Prandtl number melt during alloy solidification—*Current Topics in Crystal Growth Research* **5**, 151–161 (2000)	July 1999
915	Adrian, R. J.	On the physical space equation for large-eddy simulation of inhomogeneous turbulence—*Physics of Fluids* (submitted)	July 1999
916	Riahi, D. N.	Wave and vortex generation and interaction in turbulent channel flow between wavy boundaries—*Journal of Mathematical Fluid Mechanics* (submitted)	July 1999
917	Boyland, P. L., M. A. Stremler, and H. Aref	Topological fluid mechanics of point vortex motions	July 1999
918	Riahi, D. N.	Effects of a vertical magnetic field on chimney convection in a mushy layer—*Journal of Crystal Growth* **216**, 501–511 (2000)	Aug. 1999
919	Riahi, D. N.	Boundary mode–vortex interaction in turbulent channel flow over a non-wavy rough wall—*Proceedings of the Royal Society of London A*, in press (2001)	Sept. 1999
920	Block, G. I., J. G. Harris, and T. Hayat	Measurement models for ultrasonic nondestructive evaluation—*IEEE Transactions on Ultrasonics, Ferroelectrics, and Frequency Control* **47**, 604–611 (2000)	Sept. 1999
921	Zhang, S., and K. J. Hsia	Modeling the fracture of a sandwich structure due to cavitation in a ductile adhesive layer—*Journal of Applied Mechanics* (submitted)	Sept. 1999

List of Recent TAM Reports (cont'd)

No.	*Authors*	*Title*	*Date*
922	Nimmagadda, P. B. R., and P. Sofronis	Leading order asymptotics at sharp fiber corners in creeping-matrix composite materials	Oct. 1999
923	Yoo, S., and D. N. Riahi	Effects of a moving wavy boundary on channel flow instabilities—*Theoretical and Computational Fluid Dynamics* (submitted)	Nov. 1999
924	Adrian, R. J., C. D. Meinhart, and C. D. Tomkins	Vortex organization in the outer region of the turbulent boundary layer—*Journal of Fluid Mechanics* **422**, 1–53 (2000)	Nov. 1999
925	Riahi, D. N., and A. T. Hsui	Finite amplitude thermal convection with variable gravity—*International Journal of Mathematics and Mathematical Sciences* **25**, 153–165 (2001)	Dec. 1999
926	Kwok, W. Y., R. D. Moser, and J. Jiménez	A critical evaluation of the resolution properties of *B*-spline and compact finite difference methods—*Journal of Computational Physics* (submitted)	Feb. 2000
927	Ferry, J. P., and S. Balachandar	A fast Eulerian method for two-phase flow—*International Journal of Multiphase Flow*, in press (2000)	Feb. 2000
928	Thoroddsen, S. T., and K. Takehara	The coalescence–cascade of a drop—*Physics of Fluids* **12**, 1257–1265 (2000)	Feb. 2000
929	Liu, Z.-C., R. J. Adrian, and T. J. Hanratty	Large-scale modes of turbulent channel flow: Transport and structure—*Journal of Fluid Mechanics* (submitted)	Feb. 2000
930	Borodai, S. G., and R. D. Moser	The numerical decomposition of turbulent fluctuations in a compressible boundary layer—*Theoretical and Computational Fluid Dynamics* (submitted)	Mar. 2000
931	Balachandar, S., and F. M. Najjar	Optimal two-dimensional models for wake flows—*Physics of Fluids*, in press (2000)	Mar. 2000
932	Yoon, H. S., K. V. Sharp, D. F. Hill, R. J. Adrian, S. Balachandar, M. Y. Ha, and K. Kar	Integrated experimental and computational approach to simulation of flow in a stirred tank—*Chemical Engineering Sciences* (submitted)	Mar. 2000
933	Sakakibara, J., Hishida, K., and W. R. C. Phillips	On the vortical structure in a plane impinging jet—*Journal of Fluid Mechanics* **434**, 273–300 (2001)	Apr. 2000
934	Phillips, W. R. C.	Eulerian space–time correlations in turbulent shear flows	Apr. 2000
935	Hsui, A. T., and D. N. Riahi	Onset of thermal–chemical convection with crystallization within a binary fluid and its geological implications—*Geochemistry, Geophysics, Geosystems* **2**, 2000GC000075 (2001)	Apr. 2000
936	Cermelli, P., E. Fried, and S. Sellers	Configurational stress, yield, and flow in rate-independent plasticity—*Proceedings of the Royal Society of London A* **457**, 1447–1467 (2001)	Apr. 2000
937	Adrian, R. J., C. Meneveau, R. D. Moser, and J. J. Riley	Final report on 'Turbulence Measurements for Large-Eddy Simulation' workshop	Apr. 2000
938	Bagchi, P., and S. Balachandar	Linearly varying ambient flow past a sphere at finite Reynolds number—Part 1: Wake structure and forces in steady straining flow	Apr. 2000
939	Gioia, G., A. DeSimone, M. Ortiz, and A. M. Cuitiño	Folding energetics in thin-film diaphragms	Apr. 2000
940	Chaïeb, S., and G. H. McKinley	Mixing immiscible fluids: Drainage induced cusp formation	May 2000
941	Thoroddsen, S. T., and A. Q. Shen	Granular jets—*Physics of Fluids* **13**, 4–6 (2001)	May 2000
942	Riahi, D. N.	Non-axisymmetric chimney convection in a mushy layer under a high-gravity environment—In *Centrifugal Materials Processing* (L. L. Regel and W. R. Wilcox, eds.), 295–302 (2001)	May 2000

List of Recent TAM Reports (cont'd)

No.	*Authors*	*Title*	*Date*
943	Christensen, K. T., S. M. Soloff, and R. J. Adrian	PIV Sleuth: Integrated particle image velocimetry interrogation / validation software	May 2000
944	Wang, J., N. R. Sottos, and R. L. Weaver	Laser induced thin film spallation—*Experimental Mechanics* (submitted)	May 2000
945	Riahi, D. N.	Magnetohydrodynamic effects in high gravity convection during alloy solidification—In *Centrifugal Materials Processing* (L. L. Regel and W. R. Wilcox, eds.), 317–324 (2001)	June 2000
946	Gioia, G., Y. Wang, and A. M. Cuitiño	The energetics of heterogeneous deformation in open-cell solid foams	June 2000
947	Kessler, M. R., and S. R. White	Self-activated healing of delamination damage in woven composites—*Composites A: Applied Science and Manufacturing* **32**, 683–699 (2001)	June 2000
948	Phillips, W. R. C.	On the pseudomomentum and generalized Stokes drift in a spectrum of rotational waves—*Journal of Fluid Mechanics* **430**, 209–229 (2001)	July 2000
949	Hsui, A. T., and D. N. Riahi	Does the Earth's nonuniform gravitational field affect its mantle convection?—*Physics of the Earth and Planetary Interiors* (submitted)	July 2000
950	Phillips, J. W.	Abstract Book, 20th International Congress of Theoretical and Applied Mechanics (27 August – 2 September, 2000, Chicago)	July 2000
951	Vainchtein, D. L., and H. Aref	Morphological transition in compressible foam—*Physics of Fluids* **13**, 2152–2160 (2001)	July 2000
952	Chaïeb, S., E. Sato-Matsuo, and T. Tanaka	Shrinking-induced instabilities in gels	July 2000
953	Riahi, D. N., and A. T. Hsui	A theoretical investigation of high Rayleigh number convection in a nonuniform gravitational field—*Acta Mechanica* (submitted)	Aug. 2000
954	Riahi, D. N.	Effects of centrifugal and Coriolis forces on a hydromagnetic chimney convection in a mushy layer—*Journal of Crystal Growth* **226**, 393–405 (2001)	Aug. 2000
955	Fried, E.	An elementary molecular-statistical basis for the Mooney and Rivlin–Saunders theories of rubber-elasticity—*Journal of the Mechanics and Physics of Solids*, in press (2001)	Sept. 2000
956	Phillips, W. R. C.	On an instability to Langmuir circulations and the role of Prandtl and Richardson numbers—*Journal of Fluid Mechanics*, in press (2001)	Sept. 2000
957	Chaïeb, S., and J. Sutin	Growth of myelin figures made of water soluble surfactant—Proceedings of the 1st Annual International IEEE–EMBS Conference on Microtechnologies in Medicine and Biology (October 2000, Lyon, France), 345–348	Oct. 2000
958	Christensen, K. T., and R. J. Adrian	Statistical evidence of hairpin vortex packets in wall turbulence—*Journal of Fluid Mechanics* **431**, 433–443 (2001)	Oct. 2000
959	Kuznetsov, I. R., and D. S. Stewart	Modeling the thermal expansion boundary layer during the combustion of energetic materials—*Combustion and Flame*, in press (2001)	Oct. 2000
960	Zhang, S., K. J. Hsia, and A. J. Pearlstein	Potential flow model of cavitation-induced interfacial fracture in a confined ductile layer—*Journal of the Mechanics and Physics of Solids* (submitted)	Nov. 2000
961	Sharp, K. V., R. J. Adrian, J. G. Santiago, and J. I. Molho	Liquid flows in microchannels—Chapter 6 of *CRC Handbook of MEMS* (M. Gad-el-Hak, ed.) (2001)	Nov. 2000
962	Harris, J. G.	Rayleigh wave propagation in curved waveguides—*Wave Motion*, in press (2001)	Jan. 2001
963	Dong, F., A. T. Hsui, and D. N. Riahi	A stability analysis and some numerical computations for thermal convection with a variable buoyancy factor—*Geophysical and Astrophysical Fluid Dynamics* (submitted)	Jan. 2001

List of Recent TAM Reports (cont'd)

No.	*Authors*	*Title*	*Date*
964	Phillips, W. R. C.	Langmuir circulations beneath growing or decaying surface waves—*Journal of Fluid Mechanics* (submitted)	Jan. 2001
965	Bdzil, J. B., D. S. Stewart, and T. L. Jackson	Program burn algorithms based on detonation shock dynamics—*Journal of Computational Physics* (submitted)	Jan. 2001
966	Bagchi, P., and S. Balachandar	Linearly varying ambient flow past a sphere at finite Reynolds number: Part 2—Equation of motion—*Journal of Fluid Mechanics* (submitted)	Feb. 2001
967	Cermelli, P., and E. Fried	The evolution equation for a disclination in a nematic fluid—*Proceedings of the Royal Society A*, in press (2001)	Apr. 2001
968	Riahi, D. N.	Effects of rotation on convection in a porous layer during alloy solidification—Chapter in *Transport Phenomena in Porous Media* (D. B. Ingham and I. Pop, eds.), Oxford: Elsevier Science (2001)	Apr. 2001
969	Damljanovic, V., and R. L. Weaver	Elastic waves in cylindrical waveguides of arbitrary cross section—*Journal of Sound and Vibration* (submitted)	May 2001
970	Gioia, G., and A. M. Cuitiño	Two-phase densification of cohesive granular aggregates	May 2001
971	Subramanian, S. J., and P. Sofronis	Calculation of a constitutive potential for isostatic powder compaction—*International Journal of Mechanical Sciences* (submitted)	June 2001
972	Sofronis, P., and I. M. Robertson	Atomistic scale experimental observations and micromechanical/continuum models for the effect of hydrogen on the mechanical behavior of metals—*Philosophical Magazine* (submitted)	June 2001
973	Pushkin, D. O., and H. Aref	Self-similarity theory of stationary coagulation—*Physics of Fluids* (submitted)	July 2001
974	Lian, L., and N. R. Sottos	Stress effects in ferroelectric thin films—*Journal of the Mechanics and Physics of Solids* (submitted)	Aug. 2001
975	Fried, E., and R. E. Todres	Prediction of disclinations in nematic elastomers—*Proceedings of the National Academy of Sciences*, in press (2002)	Aug. 2001
976	Fried, E., and V. A. Korchagin	Striping of nematic elastomers—*International Journal of Solids and Structures*, in press (2002)	Aug. 2001
977	Riahi, D. N.	On nonlinear convection in mushy layers: Part I. Oscillatory modes of convection—*Journal of Fluid Mechanics* (submitted)	Sept. 2001
978	Sofronis, P., I. M. Robertson, Y. Liang, D. F. Teter, and N. Aravas	Recent advances in the study of hydrogen embrittlement at the University of Illinois—Invited paper, Hydrogen–Corrosion Deformation Interactions (Sept. 16–21, 2001, Jackson Lake Lodge, Wyo.)	Sept. 2001
979	Fried, E., M. E. Gurtin, and K. Hutter	A void-based description of compaction and segregation in flowing granular materials—*Proceedings of the Royal Society of London A* (submitted)	Sept. 2001
980	Adrian, R. J., S. Balachandar, and Z.-C. Liu	Spanwise growth of vortex structure in wall turbulence—Korean Society of Mechanical Engineers special issue on Flow Visualization (December 2001)	Sept. 2001
981	Adrian, R. J.	Information and the study of turbulence and complex flow—*Japanese Society of Mechanical Engineers B* (submitted)	Oct. 2001
982	Adrian, R. J., and Z.-C. Liu	Observation of vortex packets in direct numerical simulation of fully turbulent channel flow—*Journal of Visualization* (submitted)	Oct. 2001
983	Fried, E., and R. E. Todres	Disclinated states in nematic elastomers—*Journal of the Mechanics and Physics of Solids* (submitted)	Oct. 2001
984	Stewart, D. S.	Towards the miniaturization of explosive technology—Proceedings of the 23rd International Conference on Shock Waves (2001)	Oct. 2001
985	Stewart, D. S.	Spinning instability of gaseous detonations—*Journal of Fluid Mechanics* (submitted)	Oct. 2001
986	Brown, E. N., N. R. Sottos, and S. R. White	Fracture testing of a self-healing polymer composite—*Experimental Mechanics* (submitted)	Nov. 2001